

## ON THE INCREASE OF ULTRAVIOLET RADIATION DETECTION EFFICIENCY IN NUCLEAR PARTICLE DETECTORS WITH THE HELP OF TRANSPARENT WAVELENGTH SHIFTER FILMS

A.M. GORIN, G.D. KAKAURIDZE, A.I. PERESYPKIN, V.A. POLYAKOV, V.I. RYKALIN  
and E.G. TZHADADZE

*Institute for High Energy Physics, Serpukhov, USSR*

Received 29 October 1985 and in revised form 22 April 1986

The performance of transparent wavelength shifters (WLS) on the base of polymethylmethacrylate and organic luminophors has been studied. Measurements have been carried out in the near and far ultraviolet. Using multicomponent WLS covering the photomultiplier (PM) window, the maximum quantum efficiency of the PM photocathode was increased up to 30%. Due to the use of WLS in the gas Cherenkov counter (radiator Fr-12) a photoelectric efficiency 2.3 times higher than for FEU-110 has been obtained. Now the FEU-110 photoelectric efficiency equals to photoelectric efficiency of the 56DUVP PM.

### 1. Introduction

The efficiency of light radiation registration determines the main characteristics of a number of particle detectors. For scintillation counters and hodoscopes this efficiency is decisive for the choice of scintillator thickness, i.e. the amount of matter along the particle path, and ultimate hodoscope spatial resolution. The number of Cherenkov photons emitted per unit wavelength depends on the wavelength and is defined by the formula  $dN/d\lambda \sim 1/\lambda^2$ , thus it is very important for Cherenkov counters to detect ultraviolet radiation with high efficiency. The shortwave limit for the transmission of gases usually used as radiators lies below 150 nm for He, Ne, Ar, and for N<sub>2</sub>, CO<sub>2</sub>, most of the freons and hydrocarbons it is within the range of 150–240 nm [1]. Therefore high detection efficiency of Cherenkov radiation may be achieved if one uses PMs with quartz ( $\lambda \geq 180$  nm), MgF<sub>2</sub> ( $\lambda \geq 125$  nm), GaF<sub>2</sub> ( $\lambda \geq 130$  nm), or LiF ( $\lambda \geq 110$  nm) windows only a few mm thick. However, high cost and the absence of homemade PMs with photocathode diameters larger than 2–4 cm for the above materials complicate measurements in the ultraviolet wavelength region inaccessible for PMs with glass windows ( $\lambda < 350$  nm). For electroluminescence detectors such as counters, proportional and drift chambers [2–8] the energy resolution that may be achieved, loading characteristics and maximum possible sizes are determined by the efficiency of light registration. An effective way to improve a PM's sensitivity in the ultraviolet range is to use wavelength shifters (WLS) which shift the ultraviolet radiation to the wavelengths of maximum spectral sensitivity of the more common efficient photocathodes.

Vacuum evaporated WLS made from p-terphenyl (PTP) and tetraphenylbutadiene (TPB) allow a factor of 3 to 4 improvement in the efficiency of PMs with glass windows [9,10] when used with crystals and gases transmitting the light in the far ultraviolet region such as Cherenkov light radiators. In refs. [11–14] it has been shown that in the ultraviolet region ( $\lambda \geq 200$  nm) films formed on the PM photocathode windows are also quite effective. The film is composed of a PTP solution mixed with a plastic binder in an organic solvent. The sensitivity of PMs with glass windows to Cherenkov light achieved in this region increases by a factor of 2. Note that WLS films prepared by the deposition from the solvent have better mechanical properties and are easier to use than those prepared by vacuum deposition.

Normally used WLS depositions have a polycrystalline structure caused by the process of recrystallization or p-terphenyl crystallization in the films after the preparation, which results from high concentrations of p-terphenyl in the film substance. This fact restricts the applicability of such WLSs, for instance, in making UV-sensitive fibers and strips [7] as light-guide shifters for the electroluminescence chambers. In those cases WLS optical transparency is required for light propagation along the fiber. WLSs optically transparent to their own radiation are of great interest from the point of view of increasing the efficiency of radiation registration in the region where total internal reflection of the light occurs at the WLS–gas (vacuum) and photocathode–vacuum boundaries. The characteristics of such WLSs and their manufacturing techniques are described in refs. [12,14,15]. The present paper is, in fact, a generalization and further development of previous work [14,16,17]. It is devoted to the investigation of the

characteristics of transparent WLSs over a wide range including the far ultraviolet one.

## 2. Investigation of performance of transparent film wave-length shifters

Polymethylmethacrylate (PMMA) was chosen as a plastic binder in manufacturing transparent WLS films by settling them from the solvent. The reason for such a choice is the availability of this material, its transparency, and the long term stability of the manufactured films. The films were settled on polished quartz sublayers 3 mm thick with a diameter of 30 mm from PMMA and luminophor-light shifter solvent in toluene. The basic characteristics of the luminophors used are listed in table 1.

The transition and excitation spectra of the WLS films were measured with the help of the SF-26 spectrophotometer, working in the wavelength range 186–1200 nm. The light detector of the spectrophotometer was replaced by a 56 UVP PM with SbCs photocathode and a quartz window (see fig. 1). Dry nitrogen was circulated through the spectrophotometer at a positive pressure to eliminate ultraviolet radiation absorption in the region  $\lambda \leq 200$  nm.

To measure the transmission spectrum along the optical axis of the cuvette section, two samples, one with the film on a quartz plate and the other pure quartz only, whose transmission was taken to be 100%, were installed with the help of a movable bogie (8). In order to study the spectra of the luminescence excitation, a curved light guide (3) (fig. 2a) on whose lateral side a sample (7) was fixed, was installed. An optical

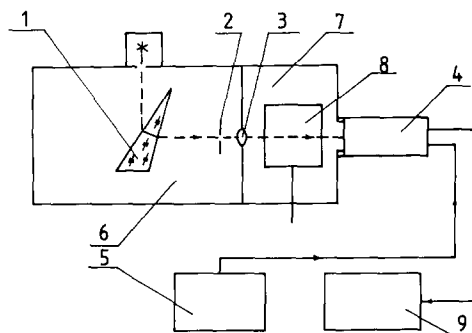


Fig. 1. The setup scheme to investigate WLS films: (1) quartz prism, (2) diaphragm, (3) quartz focusing lens, (4) 56UVP, (5) hv power supply, (6) SF-26 spectrophotometer, (7) SF-26 cuvette section, (8) movable bogie on which the samples to investigate transmission spectra were installed, (9) microammeter.

contact was made with an optical coupler between the sample and the light guide. Because of this coupling some part of the sample luminescence radiation  $J_s(\lambda)$ , created when the same was irradiated by the varying light wavelength,  $\lambda$ , of the light generator, was detected by the PM. In this case the “direct” light from the spectrophotometer monochromator was absorbed by an opaque screen (4). The PM current dependence  $J_p(\lambda)$  on the monochromator “direct” light (without light absorber) was measured separately.

These measurements allow one to obtain the relative excitation spectrum of the sample  $S(\lambda)$ :

$$S(\lambda) = \frac{J_s(\lambda)}{J_p(\lambda)\eta}, \quad (1)$$

Table 1  
Luminophor characteristics <sup>a)</sup>

No.	Luminophors	Maximum of absorption spectrum [nm]	Maximum of emission spectrum [nm]	Fluorescence quantum efficiency	Decay time [ns]
1.	PPO (2,5-Diphenyloxazole)	308	365	0.8	1.6
2.	PTP (p-Terphe-nyl)	290	360	0.85	1.2
3.	POPOP (1,4-Di-(2(5-Phenylloxazolyl))-benzene)	360	415	0.85	1.5
4.	Naphthalene	< 310	325	0.2	110
5.	Pyrazoline (1,5-diphenyl-3-stiril-pyrazoline)	390	460	–	6.0

<sup>a)</sup> All characteristics quoted were measured in toluene solvent.

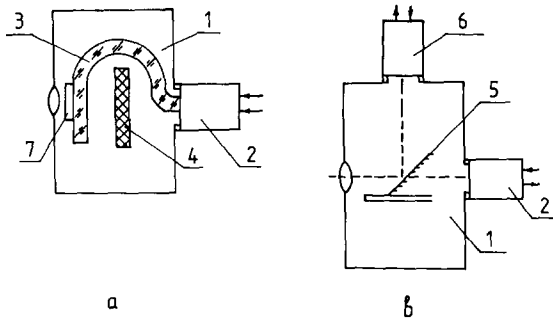


Fig. 2. Cuvette section (a) to investigate excitation spectra, (b) to measure PM quantum efficiency. (1) Cuvette section, (2) 56UVP with known quantum efficiency, (3) curved PMMA lightguide, (4) opaque screen; (5) mirror protected by a deposited layer of  $\text{MgF}_2$ , (6) photomultiplier under investigation, (7) film sample under investigation.

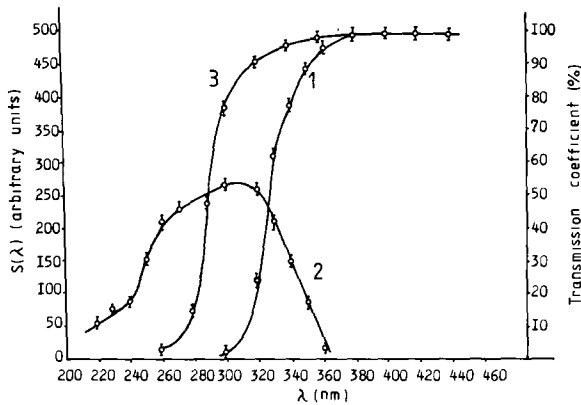


Fig. 3. Spectra of PMMA film transmission (3), transmission (1) and excitation (2) of PMMA WLS film with naphthalene at concentration  $620 \mu\text{g}/\text{cm}^2$ . Film sample thickness is  $15\text{--}20 \mu\text{m}$  in all measurements.

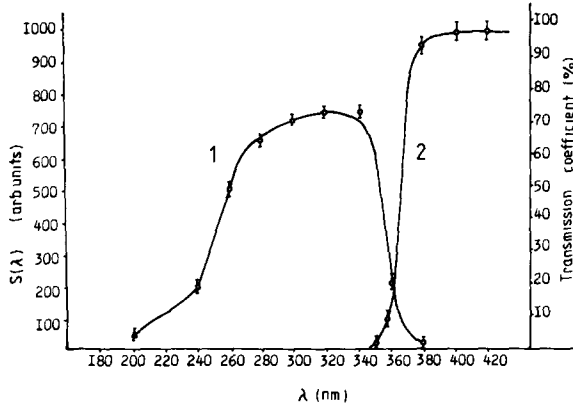


Fig. 4. Excitation (1) and transmission (2) spectra at PMMA WLS film with PPO at concentration  $200 \mu\text{g}/\text{cm}^2$ .

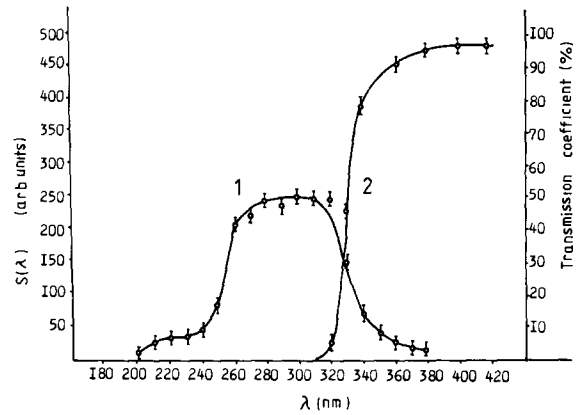


Fig. 5. Excitation (1) and transmission (2) spectra of PMMA WLS film with PTP at concentration  $45 \mu\text{g}/\text{cm}^2$ .

where  $\eta(\lambda)$  is the PM photocathode quantum efficiency.

For comparison of the transformation efficiency of the short-wavelength radiation for different WLSs use was made of the relative luminescence yield  $F$ :

$$F = A \int_{\lambda_1}^{\lambda_2} S(\lambda) d\lambda, \quad (2)$$

where  $A$  is a constant coefficient;  $\lambda_1, \lambda_2$  are the wavelengths corresponding to the excitation spectrum boundaries.

Figs. 3–5 present the excitation and transmission spectrum from pure PMMA as well as transmission spectra for films containing naphthalene, PPO, PTP. The dependences of the integral light yield  $F$  on the

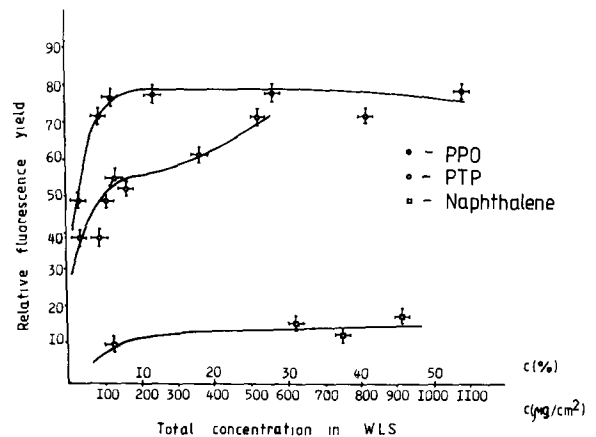


Fig. 6. Dependences of the relative luminescence yield in one-component PMMA WLS film on the luminophor concentration expressed as a percentage of PMMA weight in  $\mu\text{g}/\text{cm}^2$ .

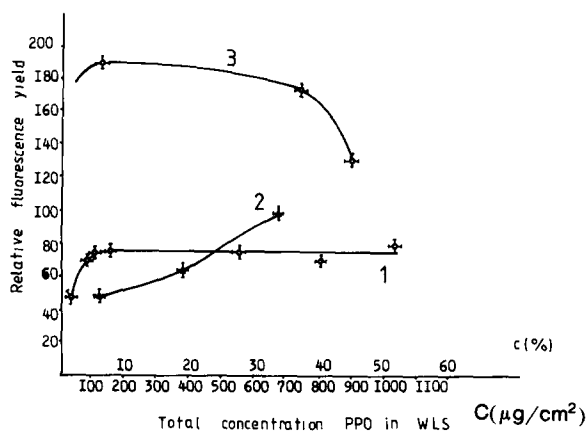


Fig. 7. Dependences of the relative luminescence yield of PMMA WLS films on PPO concentration expressed as a percentage of PMMA weight in  $\mu\text{g}/\text{cm}^2$ : (1) PPO; (2) PPO + 55  $\mu\text{g}/\text{cm}^2$  PTP (2.5%), (3) PPO + 55  $\mu\text{g}/\text{cm}^2$  PTP + 3  $\mu\text{g}/\text{cm}^2$  POPOP (0.15%).

concentration of the luminophors  $C$  in one-component WLS films are shown in figs. 6 and 7. Film samples of 15–20  $\mu\text{m}$  were used for these measurements. Note that the indicated errors in luminophor concentration refer to the scale in  $\mu\text{g}/\text{cm}^2$ , and the errors for percent (over

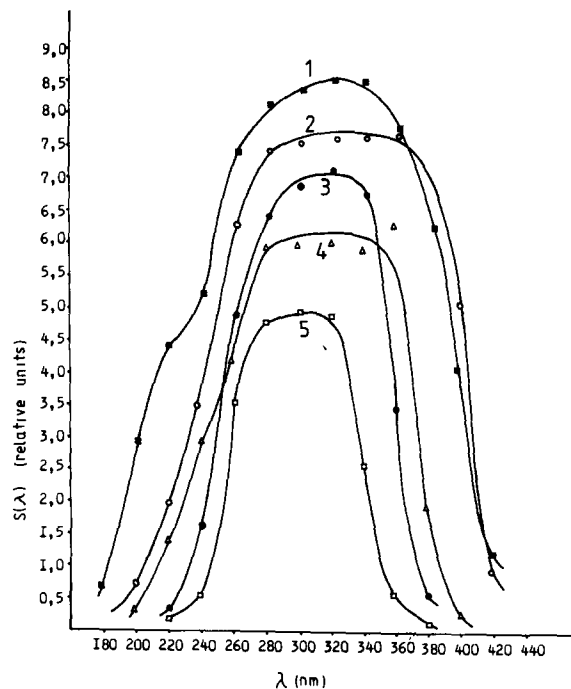


Fig. 8. Excitation spectra of PMMA WLS film at luminophor concentrations providing maximum relative luminescence yield values: (1) PPO + PTP + POPOP + naphthalene; (2) PPO + PTP + POPOP; (3) PPO; (4) PPO + PTP; (5) PTP.

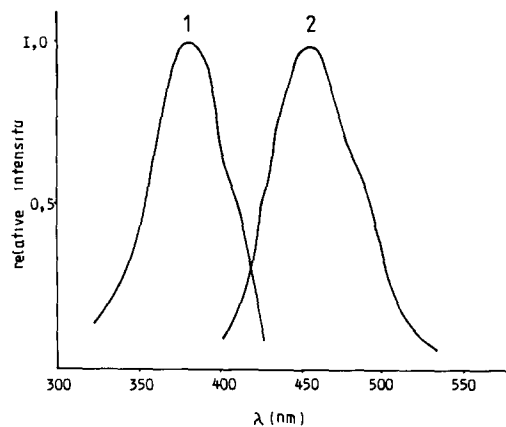


Fig. 9. Pyrazoline absorption (1) and luminescence (2) spectra.

weight) content of the luminophor in the plastic matrix are 1.5–2 times higher than the indicated ones.

From the dependences shown in fig. 6 it is seen that WLS light yield rapidly increases with PPO concentration in the region of  $C \leq 5\%$  and becomes saturated at  $C \approx 10\%$ . This saturation seems to be connected with the concentration quenching of luminescence. In the case with PTP it starts to crystallize at  $C \geq 3\%$  and the growth of the light yield at  $C > 3\%$  may be caused by changes of the PTP state of aggregation in the film. Thus the highest light yield in one-component trans-

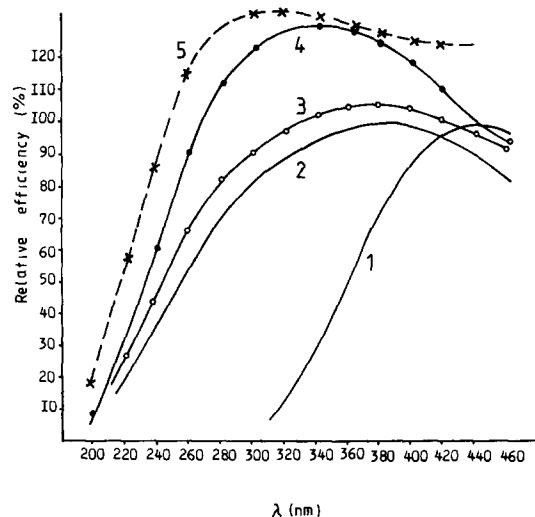


Fig. 10. Spectral dependences of PM quantum sensitivity: (1) FEU-110, maximum quantum yield  $\epsilon_{\text{max}} \approx 24\%$ ; (2) 56DUVP,  $\epsilon_{\text{max}} \approx 23\%$ ; (3) FEU-110 + WLS-film (PPO + PTP + POPOP + naphthalene); (4) FEU-110 + WLS-film (PPO + PTP + POPOP + naphthalene + pyrazoline); (5) FEU-110 + WLS, normalized to the quantum sensitivity of the 56DUVP PM,  $\epsilon_{\text{max}} \approx 24\%$ .

Table 2  
Relative WLS efficiency in vacuum ultraviolet

No.	Composition		Relative efficiency <sup>a)</sup>	Notes
1.	PTP, PMMA	1:25	$0.45 \pm 0.10$	Transparent film
2.	PTP, PMMA	1:10	$0.68 \pm 0.09$	Semitransparent PTP film crystallizing into PMMA
3.	PPO, PMMA	1:10	$0.36 \pm 0.07$	Transparent film
4.	PPO, PMMA	1:4	$0.54 \pm 0.11$	Transparent film
5.	PPO + PTP, PMMA	5:2:50	$0.74 \pm 0.12$	Transparent film
6.	PPO + PTP, PMMA	5:1:25	$0.62 \pm 0.09$	Transparent film

<sup>a)</sup> The efficiency of vacuum deposition of WLS PTP, 500  $\mu\text{g}/\text{cm}^2$ , was taken to be 1.0.

parent WLS was obtained for the films with PPO at a concentration of  $C \approx 10\%$ . Several admixtures inserted simultaneously lead to a widening of the WLS excitation spectra, this becomes clear from comparison of figs. 3–5 with fig. 8. It also follows from the dependence in fig. 8 that the largest width and highest light yield occur in the case with multicomponent WLS containing optimal concentrations of PPO, PTP, POPOP and naphthalene. Naphthalene causes a shift of the short-wave spectrum excitation boundary and, therefore, increases the light yield by 10–20%.

As compared with one-component WLS containing PPO, the light yield of the multicomponent one may be almost a factor of 2 higher (figs. 7 and 8). A further widening of the excitation spectrum and increase of the integrated light yield may be achieved by introducing pyrazoline into the WLS (fig. 10). Its absorption and luminescence spectrum in toluene solvent are given in fig. 9. Note that the pyrazoline absorption spectrum overlaps the PTP radiation spectrum and especially the PPO spectrum. Therefore, adding pyrazoline to the WLS may result in a more effective energy transfer for PTP and PPO.

The efficiency of transparent film WLSs was also measured in the vacuum ultraviolet region. A xenon resonance lamp with radiation wavelength  $\lambda = 147$  nm was used as a light source, and a 56UVP PM was used as a light receiver. A quartz plate with WLS film constituted the optical contact with the PM's window. The volume between the WLS sample and the lamp exit window was filled with dry neon at a constant flow rate. The measurement results are presented in table 2.

The data obtained make it clear that PMMA films with PPO and PTP admixtures have a high efficiency of radiation transformation in the vacuum ultraviolet region.

### 3. On increasing the Cherenkov radiation detection efficiency with transparent WLS

Three types of photocathodes, antimony caesium, bi- and trialkali are efficiently used in the visible and near

ultraviolet parts of the spectrum. When one uses the data on the photocathode spectral sensitivity from ref. [18] and through numerical integration defines the relative number of photoelectrons produced by Cherenkov radiation from photocathodes of the three types mentioned, then results will be obtained for glass and quartz windows as given in table 3. From the quoted data it is clear that Cherenkov light is detected most efficiently with bi-alkali photocathodes due to their higher quantum yield in the region of  $\lambda \leq 430$  nm. However, for homemade PMs with photocathode diameters of more than 30 mm the multialkali photocathodes (FEU-110, FEU-49) are more popular than the bi-alkali photocathodes. Therefore the aim of the present work is to make PMs with multialkali photocathodes more sensitive to Cherenkov radiation.

Using the results described in the previous section we have produced transparent WLS deposited from solution right onto the PM window surface. The spectral dependence of the quantum yield of a PM, measured with the SF-26 spectrophotometer and a standard 56UVP PM with a known quantum yield, is shown in fig. 10. As is seen from the data, transparent WLSs make it possible to widen the spectrum sensitivity range of PMs and to increase considerably the maximum quantum yield. In the case of WLS film containing 10% naphthalene, 2% PTP, 10% PPO, 0.1% POPOP, 0.1% pyrazoline, the maximum of the spectrum sensitivity shifts into the region of 320–340 nm. In this case the maximum quantum yield in this region turns out to be 30% higher than the quantum yield of the PM without WLS ( $\lambda_{\text{max}} = 440$  nm).

Table 3  
Relative number of photoelectrons produced by Cherenkov radiation

Photocathode windows	Photocathode material		
	Antimony caesium	Bialkali	Multialkali
Glass	0.64	1	0.81
Quartz	1.6	2.28	1.92

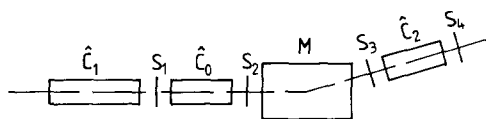


Fig. 11. The setup scheme to detect PM Cherenkov radiation efficiency.

The efficiency of applying WLS was also studied. The experimental setup is shown in fig. 11. Scintillation counters  $S_1$ – $S_4$  and gas Cherenkov counters  $C_1$  and  $C_2$  were used for muon selection. The PMs with/without WLS were installed in the third threshold counter  $C_0$ . The electromagnet  $M$  is used to analyze the events.

The counter  $C_0$ , consisting of a 1.5 m tube with a 16 cm diameter, flat mirror, and a quartz lens, was filled with freon-12 at 1 atm pressure. The short-wavelength limit of the freon-12 transmission spectrum is  $\lambda \approx 230$  nm [1].

In the measurements the amplitude spectra of PM signals (fig. 12) were recorded. Then the mean number of photoelectrons emitted from the PM photocathode was calculated. The data obtained are listed in table 4.

From the calculations taking into account the spectral distribution of Cherenkov radiation from the radiator and for the sensitivity of the FEU-110 with WLS (fig. 10) we can conclude that an optimal WLS increases the number of photoelectrons  $G = 2.6$  times. If the dependence of the reflectance of the flat mirror on the wavelength is taken into account, then  $G$  would be 2.3. This is in a good agreement with the experimentally measured results which are 2.17 (the value averaged over measurements on three PMs). The calculations also show that if air or freon-13 are used as a radiator, the expected gain factor should be  $G = 2.7$ – $2.8$ .

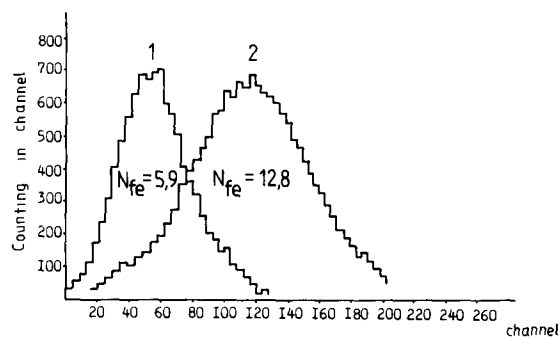


Fig. 12. FEU-110 amplitude signal spectra: (1) without WLS film, (2) PM + WLS-film (PPO + PTP + POPOP + naphthalene + pyrazoline).

#### 4. Discussion

Now we shall consider the principles involved in a transparent film WLS with PMMA deposited onto the flat PM input window. Let the area of the PM window covered with WLS be considerably larger than the window thickness. The index of refraction of the PM glass window ( $n_2$ ) and of WLS ( $n_1$ ) are approximately the same, i.e., the light in the WLS is not lost due to total internal reflection.

When the index of refraction of the photocathode is:  $n_3 > n_2$ , it does not influence the light propagation conditions at all because of total internal reflection in the system WLS–PM window. Indeed, for photons emitted by the WLS and impinging on the boundary surface WLS–gas ( $n = 1$ ) at the total internal reflection angle,  $\sin \phi_c \approx 1/n_1$ , the conditions of total internal reflection occur. This also applies to the photocathode–vacuum boundary. In this system the incident angles (on the boundary surface) do not change

Table 4

Average number of photoelectrons produced by Cherenkov light in freon-12 for different types of PMs

No.	PM type	Photo-cathode effic.	Number of photo electrons $N_0$	Ratio $G = \frac{N_0^{WLS}}{N_0}$	Sensitivity factor
1.	56 UVP	0.23	10.8		1.0
2.	56 DUVP	0.24	15.1		1.4
3.	FEU-110	0.24	8.2		0.75
	FEU-110 + WLS	0.24	16.7	2.04	1.55
4.	FEU-110	0.21	6.2		0.57
	FEU-110 + WLS	0.21	14.3	2.3	1.33
5.	FEU-110	0.18	5.9		0.54
	FEU-110 + WLS	0.18	12.8	2.1	1.19

when the light propagates along the system WLS–window–photocathode interfaces. Some fraction of light hitting the photocathode once and leaving the system through the two boundaries – through the vacuum and gas, respectively, according to ref. [20], is given by

$$f = \frac{1}{2} \left[ 1 - \left( 1 - 1/n^2 \right)^{1/2} \right], \quad (3)$$

where  $n = 1/n_2$ . The boundary surface WLS–gas is passed by a fraction of light  $f$ , which does not hit the photocathode. The rest of the light  $1-2f$ , going through the photocathode many times, will attenuate due to active photoemission and not to active absorption in the system.

For the lower limit estimate of the effective quantum yield of the photocathode of the following expression is valid:

$$\epsilon_e^1 = \left[ \epsilon(1-2d)(1 + e^{-t/t_0} + e^{-(t/t_0)^2} + \dots + e^{-(t/t_0)^n}) + f\epsilon \right] \eta, \quad (4)$$

under the assumption that all photons pass in the photocathode the distance  $t$  equal to the photocathode thickness. In this expression  $t_0$  and  $\epsilon$  are the absorption length and quantum efficiency of the PM, respectively, averaged over the WLS emission spectrum;  $\eta$  is the quantum yield of luminescence.

From eq. (4) it follows

$$\epsilon_e^1 = \left[ (1-2f) \frac{\epsilon}{1 - e^{-t/t_0}} + f\epsilon \right] \eta. \quad (5)$$

Using the data from ref. [21], valid for the region 200–400 nm, we obtain

$$\frac{\epsilon}{1 - e^{-t/t_0}} = 2\epsilon. \quad (6)$$

In the case considered  $f = 0.127$  and  $\eta \approx 0.8$ , consequently  $\epsilon_e^1 \approx 1.3\epsilon$ , i.e.

$$\epsilon_e \geq 1.3\epsilon. \quad (7)$$

This estimate of  $\epsilon_e$  does not contradict the experimentally measured value for the increase (due to the WLS) of the maximum quantum efficiency of the multi-alkali photocathode which is 30%. As noted, the values of the increase of the photoelectron number  $G$ , in their turn, agree well with those obtained from the measured spectral dependence of the PM with WLS quantum efficiency and with measurements of Cherenkov radiation detection efficiency.

The comparison of the results obtained with known data [10,11,15] on WLS application is somewhat difficult. Indeed, in the case of Cherenkov radiation detection, the efficiency of applying WLS depends on the transmission efficiency of such optical units of the Cherenkov counters as focusing lenses and input windows of PMs. Besides, an uncertainty in the results is introduced by the dependence of the photoelectron

collection efficiency of the first dynode due to the wavelength of the incident light. In ref. [11] it has been shown that different types of PMs with glass windows and identical sizes of photocathodes and the same WLS give quite different (more than two times) values for  $G$ , the signal amplification. Therefore, the value  $G$  is not sufficient to make a proper choice of a PM–WLS pair. For example, in ref. [11] the measured values for  $G$  varied, depending on the PM type (glass windows) from 1.4 to 1.8 for almost equal numbers of photoelectrons (radiator – air at 1 atm) described by the equation:

$$N = N_0 I \sin^2 \theta, \quad (8)$$

where  $N$  is the number of photoelectrons emitted from the PM photocathode when detecting Cherenkov radiation;  $L$  is the length of the Cherenkov radiator in cm;  $\theta$  is the Cherenkov radiation angle. Under the conditions from ref. [11] the value of  $N_0$  was 180. At the same time in ref. [10] the value obtained for  $G$  was 2.5 for  $N_0 = 170$ , the mirror reflection coefficient being considerably higher for this work and with the same radiator (air). Therefore it seems to us that it would be more correct to compare the Cherenkov radiation or the light from the monochromator detection efficiency with PM–WLS and PM with the known quantum sensitivity.

Fig. 10 in sect. 2 presents the spectral sensitivity dependence of the PM with WLS, normalized to the 56DUVP PM quantum yield. Both PMs have almost similar quantum yields at the sensitivity maxima. This quantum yield was  $\epsilon = 24\%$ . From this we conclude that in the region of  $\lambda \geq 250$  nm the FEU-110 PM with WLS has a larger quantum yield than the 56DUVP PM with quartz window, and in the region of 300–320 nm it is better by almost 30%. In addition a small excess of photoelectrons is emitted from the FEU-110 with WLS photocathode when compared with the 56DUVP PM. This has been experimentally confirmed. The corresponding value of  $N_0$  with freon-12 as a radiator (short-wave transmission boundary  $\lambda = 230$  nm) is 50.

Dependences similar to those in fig. 10 from ref. [11] show that a nontransparent WLS with PTP and paraloids (at PTP concentration  $\geq 20\%$ ) allows one to obtain an excess above the quantum yield of the PM with a quartz window of not more than 10%.

In a recent paper [15] on the study of transparent WLS characteristics another long-wave light shifting admixture of the bis-MSB type was used together with PTP. The concentration of admixtures of these materials in paraloids was optimized. As a result the authors managed to obtain 90% of the relative integral quantum efficiency using WLS and a 56DUVP PM with quartz window (in the region of 200–400 nm). No increase of the quantum efficiency of a PM with WLS as compared with the efficiency of a PM with a quartz window was observed [15], which seems to be connected with non-optimal conditions of light propagation due to total

internal reflection in the system WLS-PM window in the case of the 56DUVP PM and with a relatively small size of the photocathode.

### Acknowledgements

The authors express their gratitude to O.B. Gushchin for help in preliminary work, and to A.M. Blick, V.M. Kut'in, A.S. Solov'ev and the staff of the HIPERON setup for help in measurements.

### References

- [1] E.L. Garwin and A. Roder, Nucl. Instr. and Meth. 93 (1971) 593.
- [2] A.J.P.L. Policarpo, M.A. Alvez, M.C.M. Dos Santos and M.J.T. Carvalho, Nucl. Instr. and Meth. 102 (1972) 337.
- [3] P.E. Palmer and L.A. Bradu, Nucl. Instr. and Meth. 116 (1977) 578.
- [4] G. Charpak, S. Majewski and F. Saulh, Nucl. Instr. and Meth. 126 (1975) 381.
- [5] F.D. Vlatsky, V.A. Monich, Ye.A. Monich and V.I. Rykalin, Preprint IHEP 79-5, Serpukhov (1979).
- [6] S.V. Golovkin and V.I. Rykalin, Preprint IHEP 82-47, Serpukhov (1982).
- [7] D. Anderson and G. Charpak, CERN-EP/82-52 (1982).
- [8] V.I. Baskakov et al., Preprint IHEP 77-90, Serpukhov (1977).
- [9] E.L. Garwin, Y. Tomkiewicz and D. Jninez, Nucl. Instr. and Meth. 107 (1973) 365.
- [10] P. Baillon et al., Nucl. Instr. and Meth. 126 (1975) 13.
- [11] G. Eigen and E. Lorenz, Nucl. Instr. and Meth. 166 (1979) 165.
- [12] W. Viehmann and R. Frost, Nucl. Instr. and Meth. 167 (1979) 405.
- [13] H. Burkhardt et al., Nucl. Instr. and Meth. 184 (1981) 319.
- [14] G.D. Kakauridze, Thesis, TSU (1983).
- [15] M. Grande and G.R. Mozz, Nucl. Instr. and Meth. 215 (1983) 539.
- [16] V.S. Datzko et al., Preprint IHEP 82-58, Serpukhov (1982).
- [17] A.N. Vasiljev et al., Preprint IHEP 82-62, Serpukhov (1982).
- [18] Philips, Data handbook, Electron tubes, Part 9 (March, 1978).
- [19] G. Keil, Nucl. Instr. and Meth. 87 (1970) 111.
- [20] W.D. Gunter, G.R. Grant and S.A. Shaw, Appl. Opt. 9 (1970) 251.